



Peculiarities of latent track etching in SiO₂/Si structures irradiated with Ar, Kr and Xe ions



A. Al'zhanova^a, A. Dauletbekova^{a,*}, F. Komarov^b, L. Vlasukova^b, V. Yuvchenko^b, A. Akilbekov^a, M. Zdorovets^c

^a L.N. Gumilyov Eurasian National University, 2 Satpayev Str., 010008 Astana, Kazakhstan

^b Belarusian State University, 4 Nezavisimosti Av., 220030 Minsk, Belarus

^c Astana Branch of Institute of Nuclear Physics, 2/1 Abylaikhan Av., 010008 Astana, Kazakhstan

ARTICLE INFO

Article history:

Received 29 May 2015

Received in revised form 5 August 2015

Accepted 20 August 2015

Available online 2 September 2015

Keywords:

Amorphous SiO₂ layer

Ion tracks

Chemical etching

Channel system

ABSTRACT

The process of latent track etching in SiO₂/Si structures irradiated with ⁴⁰Ar (38 MeV), ⁸⁴Kr (59 MeV) and ¹³²Xe (133 and 200 MeV) ions has been investigated. The experimental results of SiO₂ etching in a hydrofluoric acid solution have been compared with the results of computer simulation based on the thermal spike model. It has been confirmed that the formation of a molten region along the swift ion trajectory with minimum radius of 3 nm can serve as a theoretical criterion for the reproducible latent track etching tracks in SiO₂.

© 2015 Elsevier B.V. All rights reserved.

1. Introduction

An irradiation of SiO₂/Si structures with swift heavy ions to form ion tracks in SiO₂ layers grown on silicon templates have attracted great interest in recent years. The latent tracks formed in SiO₂ along the swift ion trajectories can be transformed into a nanochannel system by means of chemical treatment in certain etchants [1–5]. The model involves the thermalization of the electronic subsystem of a solid within a time not exceeding 10^{−14} s. A few picoseconds later, the electron–phonon interaction leads to fast heating of the region along the fast ion trajectory. The process of energy transfer from the electronic to atomic subsystem of a solid is described by a system of two differential equations. The macroscopic parameters of the target material are used to calculate thermal fields. The model involves one free parameter: the electron mean free path under electron–phonon interaction λ . If the density of the energy released in electronic excitations is sufficiently high, we observe the melting of the material and the formation of a cylindrical domain with a diameter of a few nanometers – the future latent track. A few tens of picoseconds later, the melt cools to the temperature of the surrounding matrix. This approach is widely used to manufacture track membranes in polymer films. Such membranes are applied as fine filters in organic synthesis,

bioengineering and medicine. Nanoporous silicon dioxide can be used as a template to produce arrays of metal and semiconducting nanoclusters and nanotubes for nanoelectronic devices [6], as active elements of biosensors [7,8] as well as in new generation of track membranes with improved thermal and chemical resistance. Also, a nanochannel SiO₂ system can be used for the transmission of ion beams in new optics based on the interaction between the guiding beams of charged particles or quanta and the inner walls of a capillary [9].

Track etching is a threshold process. It is important to select proper irradiation conditions to ensure that each ion impact results in etched track formation. Usually, the electronic energy loss of an ion at the collision with the target $(dE/dx)_{e\,thr}$ is taken as a criterion for track etchability. For SiO₂, the threshold value of $(dE/dx)_{e\,thr}$ can vary from 4 to 1.5 keV/nm, according to different sources [1,10–12].

Recently, an alternative criterion has been suggested for track etchability. It is based on a thermal spike model which is used to describe the track formation processes in silicon dioxide [13]. According to the thermal spike model, the etchable track is formed via rapid quench of a molten liquid phase. The authors of Ref. [3] have reported that the track etching appears if the molten region radius is at least 1.6 nm whereas homogeneous etching occurs only for molten region (latent track) radii larger than 3.0 nm. The experimental verification of this track etchability criterion is one of the objectives set for our research.

* Corresponding author.

2. Experimental

KDB 12 (p-type silicon doped with boron) silicon substrate of 100 mm in diameter, with crystal lattice orientation (100), was subjected to wet oxygen oxidation at 900 °C in order to grow an oxide layer. According to ellipsometry measurements, the oxide layer was 1 μm thick. Then, samples of 1 × 1 cm² were cut from the produced SiO₂/Si structures for further irradiation and etching of latent tracks in SiO₂ layer. The samples were irradiated on a DC-60 cyclotron (Astana, Kazakhstan) at normal beam incidence with 200 MeV ¹³²Xe, 59 MeV ⁸⁴Kr and 38 MeV ⁴⁰Ar ions under fluences 2 × 10⁸ cm⁻², 2 × 10⁹ cm⁻². Also, samples were irradiated with 133 MeV ¹³²Xe ions at 1 × 10⁹ cm⁻². To etch latent tracks, samples were treated in 4% aqueous solution of hydrofluoric acid (HF) at room temperature for 2.5–15 min – for samples irradiated with 133 MeV Xe ions, and for 6 min – for the rest of the samples. The morphology of surface and cross sections (cleaves) of etched samples was studied by scanning electron microscopy (JSM 7500F).

3. Results and discussion

Table 1 shows parameters of an ion passage through SiO₂ obtained by SRIM [14] as well as values of the molten region radius and lifetime along the ion trajectory calculated using the thermal spike model. The thermophysical parameters of SiO₂ needed for the calculations have been taken from [1], the parameter λ was 4 nm. In our simulation the SiO₂ density was taken to be 2.2 g/cm³ [15].

One can see from the Table 1 that the electronic energy loss, (dE/dx)_e, exceeds the nuclear loss, (dE/dx)_n, by a factor of hundreds. In the case of irradiation with Kr and Xe ions the calculated molten region radii exceeds 3.0 nm predicted in [1] as threshold value for homogeneous track etching. The molten region radius is 2.2 nm for SiO₂ irradiated with Ar. It is larger than threshold one to initiate track etching (1.6 nm) but below that threshold value for homogeneous track etching.

Figs. 1–4 show SEM micrographs of the surface of SiO₂/Si structures irradiated with swift ions and etched in a HF solution. One can see that the SEM data confirm the results of simulation in the frame of the thermal spike model (Table 1). For SiO₂ irradiated with Kr and Xe ions homogeneous track etching should take place, and we could expect that each swift ion creates latent track. In fact, one can see (Figs. 1–3) that the pore's diameter is nearly the same, and the pore's density corresponds to fluence for the samples irradiated with Kr and Xe. Hence, it is possible to achieve a reproducible fabrication of nanochannels with regular shape in SiO₂ layers as well as to govern the nanochannel density by means of ion fluence. A situation is different for “light” Ar ions. One can see (Fig. 4) that pores diameters vary from ~20 to 100 nm in this case. The track etching efficiency, defined as $\xi = N_p/\Phi$, where N_p is the number of pores per unit area and Φ is the fluence, does not exceed 35%. This is in perfect agreement with theoretical prediction. The molten region radius for SiO₂ irradiated with 38 MeV Ar (2.2 nm) is lower than threshold value for homogeneous track

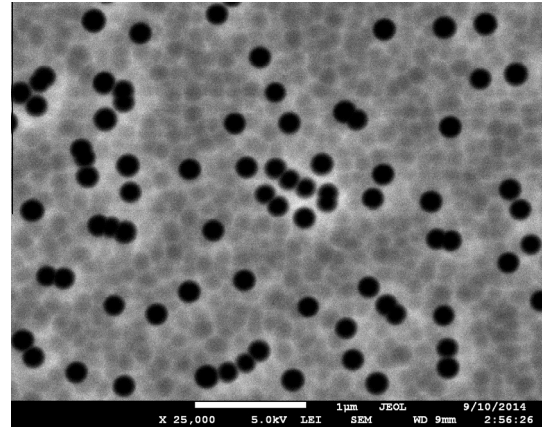


Fig. 1. The surface of the SiO₂/Si sample irradiated with Xe (133 MeV, 1 × 10⁹ cm⁻²) and etched in 4% HF solution for 5 min.

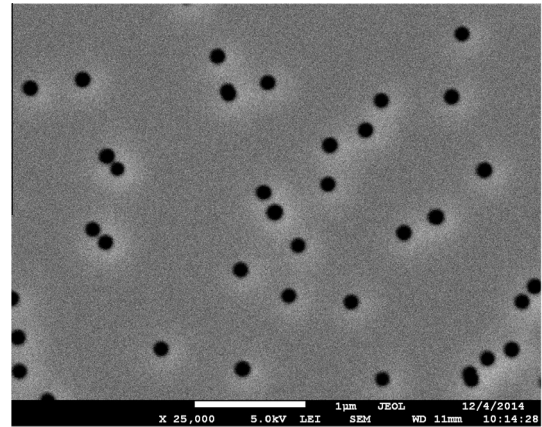


Fig. 2. The surface of the SiO₂/Si sample irradiated with Xe (200 MeV, 2 × 10⁸ cm⁻²) and etched in 4% HF solution for 6 min.

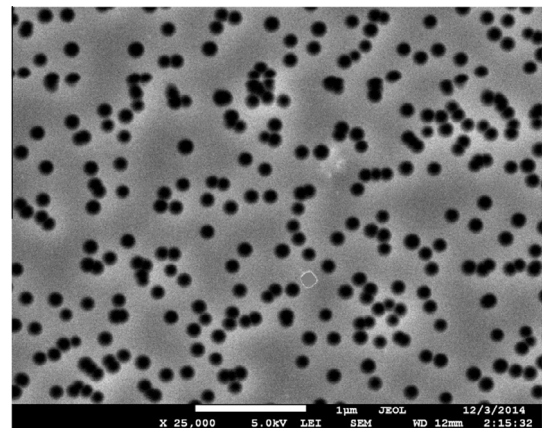


Fig. 3. The surface of the SiO₂/Si sample irradiated with Kr (59 MeV, 2 × 10⁹ cm⁻²) and etched in 4% HF solution for 6 min.

Table 1
Computer simulation results of the Xe, Kr and Ar ions passage in SiO₂.

Ion type	Ion energy, MeV	(dE/dx) _e , keV/nm	(dE/dx) _n , keV/nm	Projective range R, μm	Molten region radius r, nm	Molten region lifetime t, ps
Xe	133	13.83	0.0732	16.05	5.9	21.5
Xe	200	15.29	0.0523	20.61	6.1	23.0
Kr	59	8.8	0.0468	11.46	4.4	11.3
Ar	38	4.8	0.0101	10.79	2.2	2.7

etching (3.0 nm). Hence, we could not expect that the pore's density will amount to fluence, and the formation of pores with the same size will take place. Pores formed in silicon dioxide irradiated with Kr and Xe heavy ions have a regular conical shape (Figs. 5 and 6). This conical shape results from the comparable etching rates in the track region and in the damage-free matrix.

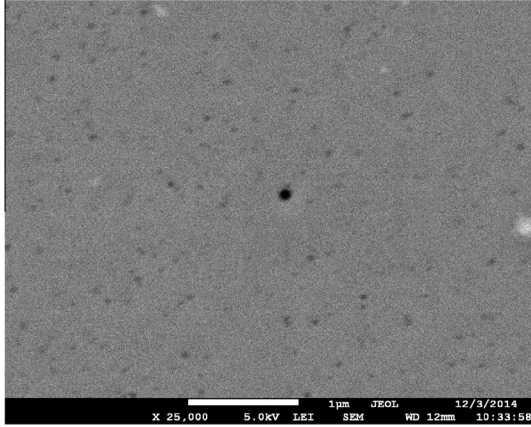


Fig. 4. The surface of the SiO₂/Si sample irradiated with Ar (38 MeV, $2 \times 10^9 \text{ cm}^{-2}$) and etched in 4% HF solution for 6 min.

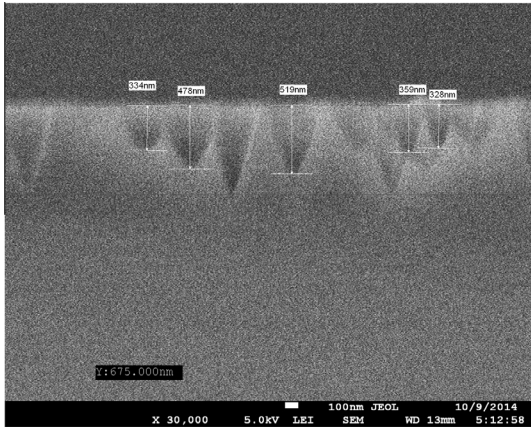


Fig. 5. The cross section of the SiO₂/Si sample irradiated with Xe (133 MeV, $1 \times 10^9 \text{ cm}^{-2}$) and etched in 4% HF solution for 10 min.

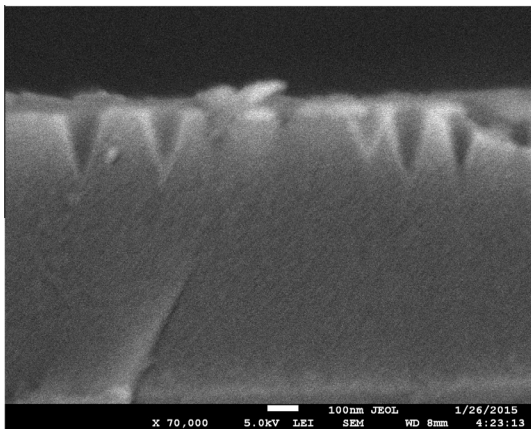


Fig. 6. The cross section of the SiO₂/Si sample irradiated with Xe (200 MeV, $2 \times 10^9 \text{ cm}^{-2}$) and etched in 4% HF solution for 6 min.

The evolution of the mean diameter of pores etched in SiO₂ at short etching times in a hydrofluoric acid solution is shown in Fig. 7.

At small etching durations, one can see nearly linear growth of the pore diameter with etching time increasing. The pore size dependence on chemical treatment duration saturates at the

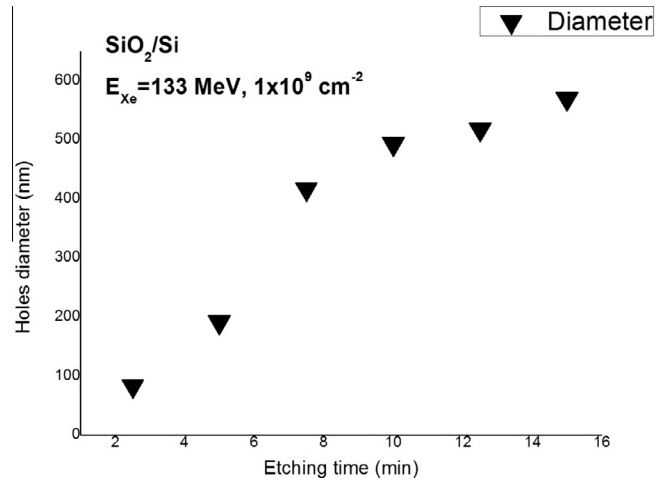


Fig. 7. The mean pore diameter in SiO₂ versus the etching time in 4% HF solution for SiO₂/Si samples irradiated with Xe ions (133 MeV, $1 \times 10^9 \text{ cm}^{-2}$).

Table 2

The mean diameter of pores (averaged over 10 measurements) in oxide layers of SiO₂/Si structures irradiated with Xe and Kr ions.

Ion	Ion energy, MeV	Etching time, min.	Fluence (Φ), cm^{-2}	Mean diameter, nm
Xe	200	6	2×10^8	127
			2×10^9	146
Kr	59	6	2×10^8	124
			2×10^9	138

etching time of 10 min. Hence, the optimum etching durations are in the range of 2 to 8 min. In this time interval the diameter of etched pores can be changed from 100 to 400 nm via increasing the etching time in HF solution.

Table 2 predicts mean diameters of pores etched in SiO₂ layers irradiated with 200 MeV Xe and 59 MeV Kr ions at fluence of 2×10^8 and $2 \times 10^9 \text{ cm}^{-2}$.

One can see noticeable increasing of the mean pore diameter with a fluence for the both types of ions. This effect is a subject of future investigation.

4. Conclusions

The formation of SiO₂ porous layers on Si substrates by irradiation of SiO₂/Si structures with Ar, Kr and Xe ions in the energy range of 38 to 200 MeV and subsequent etching in a hydrofluoric acid solution has been investigated.

The experimental etching data have been compared with the simulation results on latent track formation in amorphous silicon oxide obtained in the frame of the thermal spike model. Theoretical criterion for formation homogeneous etchable tracks in silicon oxide, namely, the formation of a molten region with radius larger than 3.0 nm [1] in the matrix along the swift ion trajectory, has been confirmed.

It has been shown that irradiation with 59 MeV Kr ions and Xe ions in the energy range of 133 to 200 MeV at a fluence of $(2 - 20) \times 10^8 \text{ cm}^{-2}$ allows to form a channel system comprising channels of regular (conical) shape with nearly the same size in amorphous SiO₂.

Acknowledgments

The study was supported by the Grant of the Ministry of Education and Science of the Republic of Kazakhstan

References

- [1] A. Dallanora, D.A. Marcondes, T.L. Bermudez, G.G. Fichtner, C. Trautmann, M. Toulemonde, R.M. Papaleo, *J. Appl. Phys.* 104 (2008) 024307.
- [2] E. Bergamini, M. Bianconi, S. Cristiani, L. Gallerani, A. Nubile, S. Petrini, S. Sugliani, *Nucl. Instrum. Methods B* 266 (2008) 2475.
- [3] L. Vlasukova, F. Komarov, V. Yuvchenko, et al., *Bull. Russ. Acad. Sci. Phys.* 76 (2012) 582.
- [4] L.A. Vlasukova, F.F. Komarov, V.N. Yuvchenko, W. Wesch, E. Wendler, A.Yu. Didyk, V.A. Skuratov, S.B. Kislitsin, *Vacuum* 5 (2014) 107.
- [5] L. Vlasukova, F. Komarov, V. Yuvchenko, A. Dauletbekova, A. Akilbekov, Simulation of latent track parameters for SiO₂ and Si₃N₄ irradiated with swift ions, in: *Materials of 5th International Conference, Radiation Interaction with Materials: Fundamentals and Applications*, Kaunas, 2014, pp. 230–234.
- [6] K. Hoppe, W. Fahrner, D. Fink, et al., *Nucl. Instrum. Methods B* 266 (2008) 1642.
- [7] M. Fujimaki, C. Rocksthul, X. Wang, et al., *Opt. Express* 16 (2008) 64068.
- [8] N. Ferting, R.H. Blick, J.C. Berhends, *J. Biophys.* 18 (2002) 3056.
- [9] N. Stolterfolt, R. Hellhammer, Z. Juhasz, et al., *Phys. Rev. A* 82 (2010) 245.
- [10] R.L. Fleischer (Ed.), *Nuclear Tracks in Solids*, Univ. California Press, Berkeley, 1975, p. 23–27.
- [11] A. Sigrist, R. Balzer, *Helv. Phys. Acta* 50 (1997) 75.
- [12] J. Jensen, M. Skupinski, A. Razpet, G. Possnert, *Nucl. Instrum. Methods B* 166/167 (2000) 903.
- [13] M. Toulemonde, A. Meftah, F. Brisard, J.M. Costantini, et al., *Phys. Rev. B: Condens. Matter* 49 (18) (1994) 12457.
- [14] SRIM code 2013 based on J.F. Ziegler, J.P. Biersak, U. Littmark, *The Stopping and Range of Ions in Solid*, Pergamon Press, New York, 1985.
- [15] *Gmelin Handbook of Inorganic and Organometallic Chemistry*, Si. Suppl. vol. B5, 8th ed., Springer-Verlag, 1994, p. 264.